

# AIRBORNE DISPERSION OF ASBESTOS FIBERS FROM SERPENTINITES: A SIMULATION ON OPHIOLITES OF PIEVESCOLA AREA (TUSCANY, ITALY)

Edoardo Zaccagnini\* and Michele Marroni\*<sup>o,✉</sup>

\* *Dipartimento di Scienze della Terra, Università di Pisa, Italy.*

<sup>o</sup> *Istituto di Geoscienze e Georisorse, CNR, Pisa, Italy.*

✉ *Corresponding author, e-mail: marroni@dst.unipi.it*

**Keywords:** *peridotites, veins, serpentine, airborne dispersion, hazard assessment. Southern Tuscany, Italy.*

## ABSTRACT

In Italy, the asbestos-related hazard is still high, mainly due to airborne dispersion of fibers as a consequence to quarrying activities into asbestos-bearing rocks, as serpentinites or basalts. The Ministerial Decree 14/05/1996 provides a method to define the hazard deriving from the exploitation of the asbestos-bearing rocks quarrying, but the proposed procedures are unclear from a geologic point of view, and not so effective for a precise hazard assessment. In this paper, we present an integrated approach based on geological, mineralogical and petrographical standard investigations on serpentinites and we test a model of airborne dispersion of fibers in order to propose more effective procedures in order to assess the asbestos-related hazard.

The adopted approach consists of 5 successive steps: 1) detailed structural mapping and collection of samples representative of the cropping out rocks, 2) petrographical study of selected thin sections of serpentinites with the aim to assess the presence of fibrous minerals, 3) X-Ray powder diffraction analyses for the identification of the species of fibrous minerals, 4) determination of the Index of Release according to the Ministerial Decree 14/05/1996 in order to determine the amount of fibrous minerals released by crushing of the asbestos-bearing serpentinites and 5) modelling of the airborne dispersion of asbestos fibers by the quarrying activity based on the data collected in the previous steps.

This approach has been simulated for an area located west of Pievescola, south of Casole d'Elsa (Southern Tuscany), where no quarrying activity occurs or is scheduled for the future. The implications of the adopted approach are also discussed in order to identify valuable procedures to minimize the asbestos-related hazard.

## INTRODUCTION

Asbestos is a group of six naturally-occurring silicate minerals (crysotile, crocidolite, amosite, tremolite, actinolite, anthophyllite), used commercially for their physical properties (e.g., Strohmeier et al., 2010). They all have in common their asbestiform habit, i.e., long, thin fibrous crystals with about 1:20 aspect ratio.

Asbestos mining began more than 4,000 years ago, but it was only at the end of the 19<sup>th</sup> century that it began as a large-scale activity. From the time of the first recorded use of asbestos by Stone Age man to 1900, the total world production was probably between  $200 \times 10^3$  and  $300 \times 10^3$  tons. However, use of asbestos greatly increased after World War I up to a maximum production for year of  $4.8 \times 10^6$  tons in 1977 (Virta, 2002). The asbestos was used for its properties as sound absorption, average tensile strength and its resistance to fire, heat, electrical and chemical damage.

In the seventies, the epidemiological researches have provided the evidences that significant exposure to any type of asbestos would increase the risk of diseases as lung cancer, mesothelioma and pleural disorders (Doll, 1955; Mossman et al., 1990; Hughes and Weill, 1991; Wagner, 1991; Cattaneo et al., 2006). This conclusion was based on observations of groups of workers with cumulative exposures to airborne concentrations of asbestos fibers. For instance, the ecological study by Marinaccio et al. (2008), based on a data set containing all lung and pleural cancer deaths in each Italian municipality in the period 1980-2001, indicates that the pleural to lung cancer ratio was estimated to be 1:1 and 3% of all male lung cancer deaths were found to be asbestos-related.

As a consequence of these problems for the human health, Italy, like as the others countries of the European Community, fully banned the use of asbestos in 1992 and set up a comprehensive plan for asbestos decommissioning in industry and housing. In Italy, the environmental risk re-

lated to asbestos is still high, mainly due to airborne dispersion of fibers as a consequence of: 1) damaging of unremoved asbestos-bearing products as, for instance, concrete, bricks, pipes and fireplace cement, and to 2) quarrying activities into asbestos-bearing rocks for ballast production, environmental clean-up of inactive quarries and excavation for works like tunnels, roads or dams.

About the second point, the Italian law, in Ministerial Decree 14/05/1996 (Italian Ministerial Decree, 1996) provides a method to define the hazard about the asbestos-bearing rocks, establishing a limit value obtained by the determination of the Index of Release (hereafter IR), i.e., the ratio of concentration of asbestos fibers liberated after abrasion tests (i.e., Bellopede et al., 2009). The same Ministerial Decree indicates, as a preliminary evaluation step, the geological evaluation of the asbestos-bearing rocks, but it does not provide accurate directives about its achievement. Moreover, no evaluation of airborne dispersion of the fibers is taken into account by the Ministerial Decree. Thus, the hazard about the asbestos-bearing rocks determined by the IR as defined in the Ministerial Decree 14/05/1996 does not seem to be effective as requested by the modern land planning.

In this paper, an integrated approach based on geological, mineralogical and petrographical investigations, jointed with a physical model of airborne dispersion of fibers, is tested in an area where serpentinites are cropping out, in order to propose a more effective method to assess the asbestos-related hazard. The implications of this approach are discussed, in order to identify valuable procedures to minimize the asbestos-related hazard.

## THE INTEGRATED APPROACH

Our integrated approach is based on several investigations with standard geological techniques that can be applied not only by researchers but also by geological consultants

and requires standard equipment that are commonly found in public and private laboratories.

The integrated approach consists of 5 successive steps, as reported hereafter.

1) Detailed structural mapping of the area where the serpentinites are cropping out. In the selected area an accurate recognition of different lithotypes has been performed together with the identification of all the asbestos-veins. The attitude of asbestos-veins, as well as their volume percentage along a length of ten meters, have been measured. The aim of this step is to collect a number of samples representative of whole outcrop for the following analyses;

2) Petrographical characterization of the selected samples, through optical microscopy. The aim of this step is to verify the presence of asbestos minerals, as well as their relative occurrence in the sample volume, either in the veins or in the groundmass wallrock for analyses by X-Ray powder Diffraction (XRPD) and IR techniques;

3) Identification by XRPD analyses of the fibrous minerals found in the selected sampled.

4) Measurement of the IR of the selected serpentinite samples, according to the procedures established by the Ministerial Decree 14/05/1996. The aim of this step is the assessment of the release of fibers by crushing of the asbestos-bearing rocks according to the law indications;

5) Model of the airborne dispersion of the asbestos fibers due to quarrying activity based the results of the petrographical, XRPD and IR determinations. The model has been constructed using a specific MATLAB r2010a program, to forecast the amount of fibers airborne dispersed, taking into account the simulated quarrying activity, the wind regime and the morphology.

The proposed approach has been tested in a selected area regarded as representative of asbestos-bearing serpentinites in central Italy. The selected area is located west of Pievescola, south of Casole d'Elsa, Southern Tuscany (Fig. 1). In this area no quarrying activity occurs or is scheduled for the future. However, several inactive small quarries or natural cliffs occur, providing good exposures of the serpentinites to be studied. In addition, this area has been selected for this study

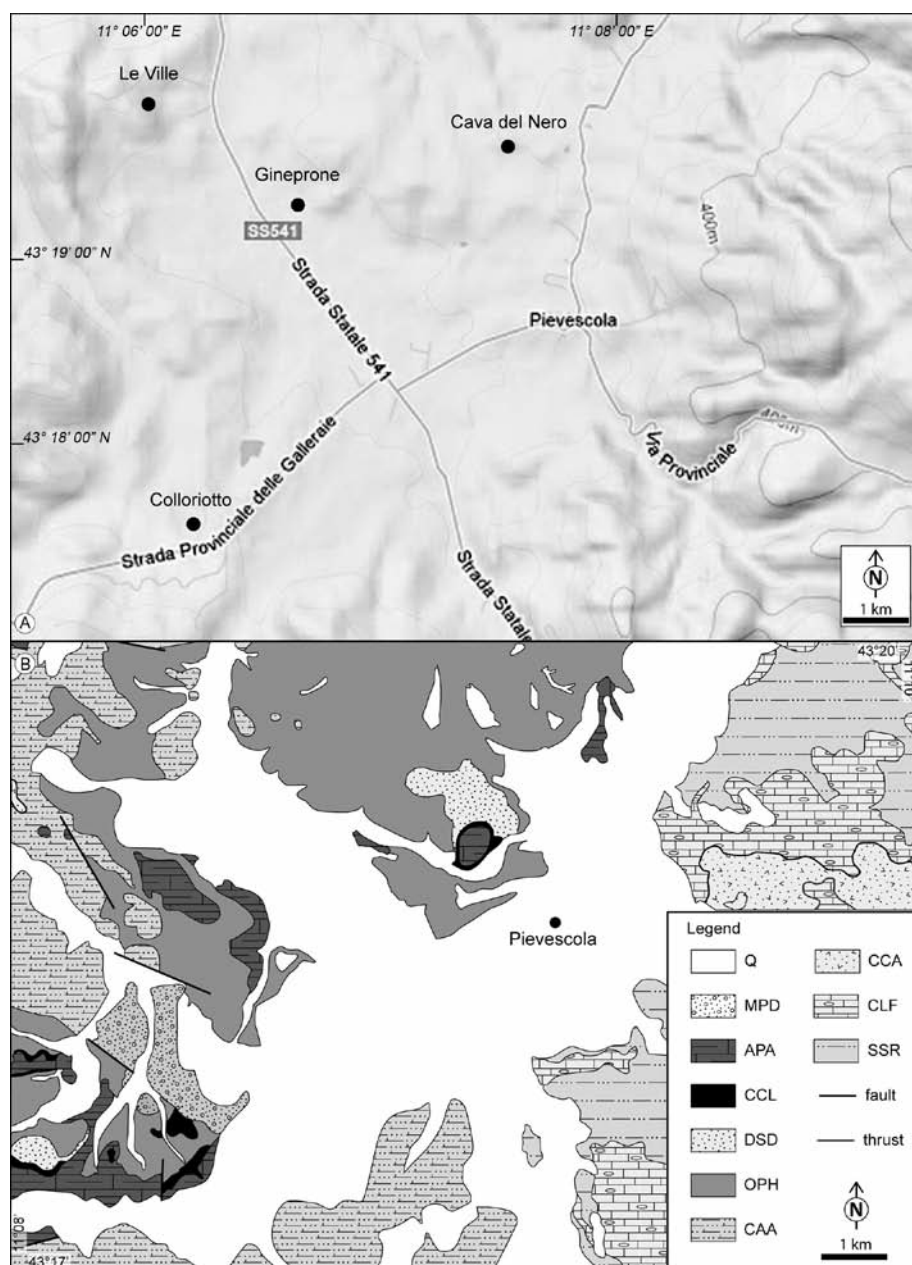


Fig. 1 - Morphology of the Pievescola area with the location of the studied outcrops (A) of serpentinites and related geological map (B). Q- Quaternary deposits; MPD- Mio-Pliocene deposits; APA- Argille a Palombini (Valanginian-Santonian); CCL- Calcari a Calpionelle (Berriasian-Valanginian); DSA- Diaspri (Callovian-Tithonian); OPH- ophiolite sequence including peridotites, gabbros and basalts (Middle-Late Jurassic); CAA- Helminthoid Flysch (Late Cretaceous); CCA- Calcare Cavernoso (Late Trias); CLF- Calcare Selcifero (Middle-Late Lias); SSR- Scisti Seritici (Aptian-Late Oligocene).

owing to its geological, morphological and the geographical features, very similar to that of the Southern Tuscany.

## THE STUDY AREA

### Geographical context

The Pievescola hamlet (lat. 67°28'58'E; long. 47°97'50'N) belongs to the Casole d'Elsa municipality (Fig. 1a). The municipality of Casole d'Elsa, placed into the Siena Province, is bounded by the municipalities of Colle Val d'Elsa, Monteriggioni, Sovicille, Chiusdino, Radicondoli, Castelnuovo Val di Cecina and Volterra. Casole d'Elsa municipality area, that covers an area of about 150 km<sup>2</sup> with a mean altitude of 417 m., includes four main hamlets: Cavallano, Mensano, Monteguidi and Pievescola. This area is crossed by two main streams: the Senna River, that flows east of Casole d'Elsa up to confluence into Elsa River North of Collalto, and the Stellate Creek, that originates from the Pilleri Mount, west of Casole d'Elsa. The latter creek flows from south to west, up to confluence with the Cecina River.

In the last decade the population has undergone a continued growth, reaching in the 31<sup>st</sup> of August of 2010, 3,862 inhabitants. In 2009 the total number of registered families is 1,593 units. The population density, with reference to 2007, is reported as 24.4 people/km<sup>2</sup>, very close to the mean value of the Siena and Grosseto Provinces. According to the Regione Toscana data (Annuario statistico regionale, 2010) concerning the use of the soil, the area of Casole d'Elsa is mainly devoted to agriculture and livestock.

The Casole d'Elsa area shows typical geomorphological features of the Southern Tuscany. This territory includes three geomorphological units (Fig. 1A) represented, respectively, by areas with predominantly hilly morphology, areas with predominantly mountainous morphology and flat areas along the valley.

The areas with predominantly hilly morphology are placed in a N-NW/S-SE trending sector north of Pievescola. It includes Casole and Cavallano areas and the little ridge between Monteguidi and Mensano. They are hilly reliefs never more than 600 m, characterized by a typical Tuscan landscape.

In the South zone, west of Pievescola, there is a higher hilly area with characteristics similar to those of mountainous zone, with an elevation of over 600 m, called "Montagnola Senese".

This area is bordered by several floodplains, characterized by a gentle gradient. These floodplains show the maximum extent in correspondence of the Elsa River and the Stellate Creek. These areas are exploited for agricultural use because of their flat morphology, and, consequently, are affected by wide landscape remodelling.

The Pievescola area, selected for this study, includes two areas with predominantly hilly morphology, connected by a narrow floodplain where the Elsa River flows. In the west side, the highest reliefs are represented by Il Poggione (336 m.) and Poggio Sermena (529 m.), whereas in the east by the Poggio Pela (282 m.), Poggio Gineprone (294 m.) and Monte Vasone (296 m.).

### Geological setting

The Casole d'Elsa area is located in the Southern Tuscany, i.e., in the central segment of the Northern Apennine

orogenic belt. This area has been selected owing the occurrence of wide areas where the Ligurian Units, that are characterized by asbestos-bearing rocks, are cropping out (Fig. 1B). The Ligurian Units are regarded as fragments of oceanic lithosphere of the Ligure-Piemontese basin that opened in the Middle Jurassic time between the Adria and Europe continental margins. These oceanic fragments were incorporated into the Apennine orogenic belt after a long-lived tectonic history that started since Late Cretaceous, as result of the convergence between the Europe and Adria plates (Marroni et al., 2010 and quoted references). The Ligurian Units are subdivided into Internal and External ones, according to the stratigraphic setting of the ophiolites. In the Internal Ligurian Units the ophiolite sequence represents the basement of a thick sedimentary cover spanning in age from Late Jurassic to Early Paleocene (Marroni and Pandolfi, 2007 and quoted references). In contrast, the External Ligurian Units are characterized by ophiolites that occur as slide block into sedimentary succession of Late Cretaceous age (Catanzariti and Perilli, 2011 and quoted references). Whereas the ophiolites from Internal Ligurian Units are representative of the oceanic lithosphere of the Ligure-Piemontese basin (Cortegno et al., 1994), those from External Ligurian Units are regarded as derived from the ocean-continent transition (Marroni et al., 2001 and quoted references).

The ophiolites from Pievescola area belong to the Internal Ligurian Units. These units are characterized by an ophiolite sequence, not thicker than 1 km, consisting of a basement made up of mantle lherzolites, intruded by gabbros and covered by a volcano-sedimentary complex, where sedimentary breccias, basaltic flows and radiolarites are complexly intermixed (Tribuzio et al., 2004 and quoted references). This stratigraphy has been interpreted as representative of an ophiolite sequence developed into a slow-spreading ridge (Treves and Harper 1994 and quoted references). In the Pievescola area the main body of the ophiolite sequence (Fig. 1B) is represented by mantle peridotites represented by spinel lherzolites with minor amount of harzburgites, both displaying tectonic porphyroclastic texture. Bands of pyroxenites are seldom observed. The mantle peridotites are intruded by small bodies of gabbros and cut by gabbro dikes, with the latter generally rodingitized. Both peridotites and gabbros are covered by ophiolitic breccias interfingering with pillow lava basalts. This ophiolite sequence is capped by pelagic/hemipelagic deposits represented by Diaspri (Callovian-Tithonian), Calcari a Calpionelle (Berriasian-Valanginian) and Argille a Palombini (Valanginian-Santonian). The Internal Ligurian Units show a polyphase deformation history (e.g., Marroni, 1991) developed under very low-grade P and T metamorphic conditions, not exceeding 3/4 kbars and 250-300°C. This deformation history has been achieved by the Internal Ligurian Units during their involvement into the Apennine orogenic history (Marroni et al., 2004 and quoted references).

## ANALYTICAL METHODS

We report here the main technical details regarding the analytical techniques used in the laboratory, i.e., XRPD analyses and the analyses for the calculation of the IR index.

XRPD analyses of 30 powdered sample of serpentinites were performed at the Dipartimento di Scienze della Terra, University of Pisa (Italy). The diffractometer used, operating in a Bragg-Brentano geometry, is composed by a Philips



PW 1830 generator, a Philips PW 1050 protractor and a Philips PW1710 electronic counting. XRPD patterns were used at working conditions as: Ni-filtered  $\text{CuK}\alpha$  radiation ( $\lambda = 0.154178$  nm), 40 KV working voltage, 20 mA working current. The acquisition program has a scanning range from  $4^\circ$  to  $65^\circ$  ( $2\theta$ ) with a step of  $0.020^\circ$  and a counting of one step per second.

IR spectrometry techniques were made on 5 samples, previously milled homogeneously to have a size from 2 to 5 cm and placed in a heater at  $400^\circ$  for an hour. After the heating and the cooling in the drier, 3 mg of sample was mixed with 300 mg of KBr, dried and milled in a mortar. Subsequently a pellet is prepared, putting the mixture in a mold of 10-30 cm of diameter, subject to a pressing of 10 tons. The resulting material is ground according the following procedures: time of autogrinding of 4 hours, a 0.45 micron porous septum to collect the powders, rotation velocity of 50 revolutions/min for the rubbing test and sieve screening gap of 1 mm. The powder is analyzed by Perkin-Elmer mod. FTIR Spectrum BX II spectrophotometer calibrated as follows: analytic range:  $4000\text{--}400$   $\text{cm}^{-1}$ , apodization: strong, resolution:  $1$   $\text{cm}^{-1}$ , number of scans of the fund: 32, number of the scans of the sample: 32.

## ANALYTICAL DATA

### Structural analyses

Four different serpentine outcrops have been examined in the Pievescola area (Fig. 2). In the field, the degree of serpentinization of the peridotites has been estimated in three classes: high (when no relics of pyroxenes or evidence of the primary texture can be detected in the field, but bastites can be always recognized at microscale), medium (when the pyroxenes are rare without evidence of primary texture) and low (when the pyroxenes are widespread and the primary texture can be seldom observed). The volume percentage of the fibrous veins has been calculated taking into account their thickness and persistence along a volume of  $10 \times 2 \times 1$  meters (Singhal and Gupta, 2010).

The outcrops are named according to the closest village or hill.

The examined outcrops are Cava del Nero (lat.  $43^\circ 19' 38''\text{N}$ ; long.  $11^\circ 07' 33''\text{E}$ ), Colloriotto (lat.  $43^\circ 17' 46''\text{N}$ ; long.  $11^\circ 05' 39''\text{E}$ ), Le Ville (lat.  $43^\circ 19' 35''\text{N}$ ; long.  $11^\circ 05' 40''\text{E}$ ) and Gineprone (lat.  $43^\circ 19' 24''\text{N}$ ; long.  $11^\circ 06' 19''\text{E}$ ).

The Cava del Nero outcrop (Fig. 2A) corresponds to an about  $50,000$   $\text{m}^2$  wide inactive quarry where serpentinized peridotites can be observed along several small but fresh quarry fronts. The peridotites are characterized by a medium degree of serpentinization with mm-sized pyroxenes well evident in the outcrop. No dunites or gabbro dikes have been found. The peridotites are cut by a complex network of veins showing a thickness ranging from 1 to 4 mm and a good lateral continuity. Each vein shows or a single or two different infillings of serpentine minerals represented by pale to dark green, massive minerals and by pale green to silvery fibers, generally growing perpendicular or subperpendicular to the vein walls; the fibrous infilling postdates everywhere the massive one. The veins occur along three systems with different attitude (Fig. 2A1): the first is about N-S trending with subvertical dipping, the second is about NE-SW with subvertical dipping, whereas the third is ENE-WSW trending with subhorizontal dipping (dipping ranging

from  $5^\circ$  to  $30^\circ$ ). In addition, very rare thick veins with a single infilling, showing a thickness from 30 to 80 mm, have been observed. The infilling is represented by pale green to silvery fibers showing well developed median lines and fibers subperpendicular to the vein walls. Cataclastic shear zones, with a thickness ranging from 10 to 80 cm, are also identified in the field (Fig. 2A2). They occur with N-S to NW-SE trending as subvertical continuous levels consisting in cm-sized fragments of peridotites in a matrix consisting of carbonate and/or of a fine-grained materials derived by crushing of peridotites. The volume percentage measurements indicate that the fibrous veins are the 1.18% of the total rock body. When both fibrous and blocky texture are coexisting in the same vein, only the first texture has been taken into account for estimation of volume percentage.

The Colloriotto outcrop (Fig. 2B) corresponds to an about  $25,000$   $\text{m}^2$  wide natural cuts along a steep cliff. The peridotites show a low degree of serpentinization, with relics of tectonic texture. No dunites or gabbro dikes have been found. The peridotites are cut by a complex network of serpentine-bearing veins showing a thickness ranging from 1 to 3 mm and a good lateral continuity along a length of about 15 m. These veins show the same features of those detected in the Cava del Nero outcrop. These veins occur along four NNW-SSE, NE-SW, E-W e NW-SE trending systems (Fig. 2B1), all with subvertical dipping except the latter system that is characterized by low dipping (dipping ranging from  $0^\circ$  to  $15^\circ$ ). Only two NW-SE trending, from 10 to 30 cm thick cataclastic shear zones (Fig. 2B2), showing similar features to those detected in the Cava del Nero, are also identified in the field. The volume percentage measurements indicate that the fibrous veins are the 0.62% of the total rock body.

The Le Ville outcrop (Fig. 2C) corresponds to an about  $40,000$   $\text{m}^2$  wide quarry fronts where serpentinized peridotites can be observed. The peridotites are characterized by a medium to low degree of serpentinization. A tectonic texture enhanced by alignments of mm-sized pyroxenes can be seldom observed. Rodingitized dikes of gabbro are widespread, whereas no dunites have been found. The peridotites are cut by a complex network of serpentine-bearing veins showing a thickness ranging from 1 to 4 mm and a good lateral continuity. These veins show the same features of those detected in the Cava del Nero and Colloriotto outcrops. These veins occur along three systems (Fig. 2C1). The first two system show subvertical dipping but different trend, ranging from NE-SE to NW-SE. The third system is characterized by NW-SE trend with subhorizontal dipping (ranging from  $10^\circ$  to  $30^\circ$ ). Few cataclastic shear zones with N-S trend and a thickness ranging from 10 to 60 cm are also identified in the field. The features are similar to those of the shear zones detected in the previous described outcrops. The rodingitized gabbro dikes consist of coarse-grained intrusive rocks with thickness ranging from 5 to 60 cm. They show a good lateral continuity, even if interrupted by faults. The gabbro dikes generally show subvertical dipping with trends ranging from NW-SE to NE-SW (Fig. 2C2). The volume percentage measurements indicate that the fibrous veins are the 0.78% of the total rock body.

The Gineprone outcrop (Fig. 2D) corresponds to an about  $10,000$   $\text{m}^2$  wide inactive quarry where serpentinized peridotites can be observed along several small quarry fronts. The peridotites are characterized by a medium degree of serpentinization, with relics of mm-sized pyroxenes and spinels. Rodingitized dikes of gabbro are widespread, whereas no dunites have been found. The peridotites are cut by a com-

plex network of serpentine-bearing veins showing a thickness ranging from 1 to 5 mm and a good lateral continuity. These veins, that show the same features of those detected in others outcrops, occur along three systems (Fig. 2D1). The first two systems show subvertical dipping but different trend, ranging from N-S to NNE-SSW. The third system is characterized by ESE-WNW trend with subhorizontal dipping (ranging from  $0^{\circ}$  to  $40^{\circ}$ ). Few cataclastic shear zones

with N-S trend and a thickness ranging from 10 to 70 cm are also identified in the field. The features are similar to those of the shear zones detected in the previous described outcrops. The rodingitized gabbro dikes consist of coarse-grained intrusive rocks with thickness ranging from 5 to 30 cm. They show the same features to those detected in the Le Ville outcrop. The gabbro dikes generally show subvertical dipping with trends ranging from N-S to NW-SE (Fig. 2D2).

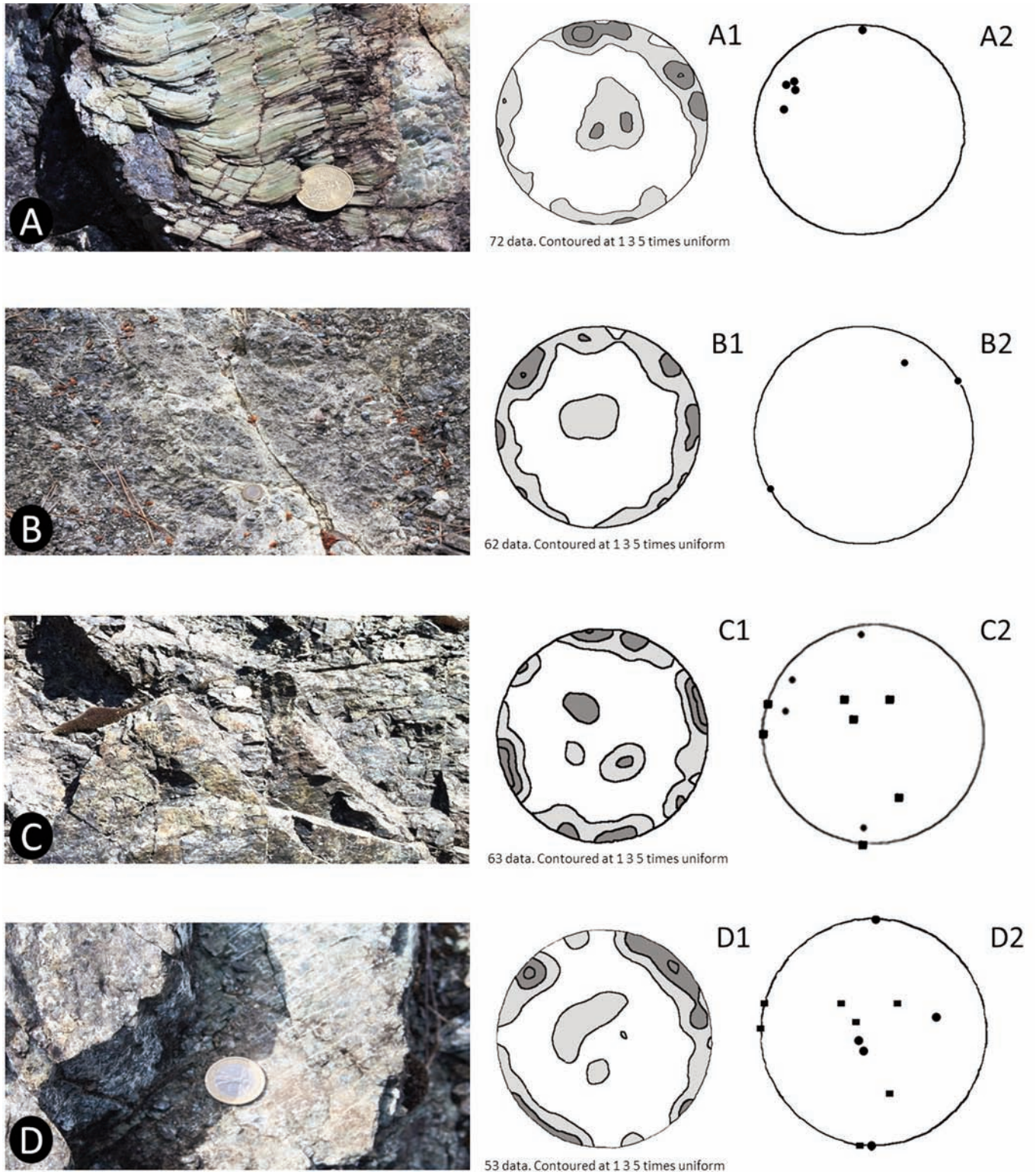


Fig. 2 - View of the outcrops (A, B, C and D), lower hemisphere projection of poles to serpentine-filled veins (A1, B1, C1 and D1) and lower hemisphere projection of poles to gabbro dykes (squares) and cataclases (dots) (A2, B2, C2, D2) of, respectively, Cava del Nero, Colloriotto, Le Ville and Gineprone outcrops.



The volume percentage measurements indicate that the fibrous veins are the 2.40% of the total rock body.

On the whole, all the studied outcrops show similar main features. The main differences are related to the serpentinization degrees as well as to the numbers of systems, thicknesses and attitudes of the veins. Differences in attitudes and thicknesses occur also for the cataclastic shear zones and the rodingitized gabbro dikes. The volume percentage measurements of the fibrous veins differ, for the studied outcrops, from 2.40% to 0.62% of the total rock body.

### Petrographical analyses

The studied serpentinites from Pievescola area can be defined as mantle peridotites, which locally include small dykes (thickness not more 30 cm) of rodingitized gabbro. A microscale petrographical and structural analyses have been performed on 12 thin sections of peridotites, plus 4 thin sections of rodingites and cataclasites.

The petrographical studies of the selected samples indicate that the peridotites can be defined as spinel lherzolites displaying tectonic porphyroclastic texture. The primary mineralogy consists of olivine and orthopyroxene, with minor amounts of clinopyroxene and spinel (Fig. 3a), generally

showing grain size smaller than that of olivine and orthopyroxene. The spinel occurs generally as interstitial phase (Fig. 3a). The peridotites show different degree of serpentinization, although orthopyroxene and spinel can be always observed as relict phases. The serpentinization of the peridotites produced both mesh and hourglass textures where serpentine replaced partially or totally the primary olivines. Serpentine minerals occur also in veins, showing both non fibrous or fibrous texture.

At the microscale, the blocky veins show a good lateral continuity with single tapering termination and are characterized by an infilling that consists of a fine-grained, not oriented minerals. Their walls are sharp without discontinuities but fragments randomly enclosed in the infilling can be observed. The blocky veins are cut by the fibrous ones, but co-existing blocky and fibrous textures in the same vein have been also observed.

The fibrous veins (Fig. 3b), show thickness change along short distance with single tapering terminations and are characterized by well-developed fibers perpendicular or sub-perpendicular to the vein walls. These veins can be defined as antitaxial type, according to Ramsay (1980). At crossed nicols, a finely spaced banding everywhere parallel to vein margins is produced by the crystallographic orientation of the different segments of the fibers. These bands,

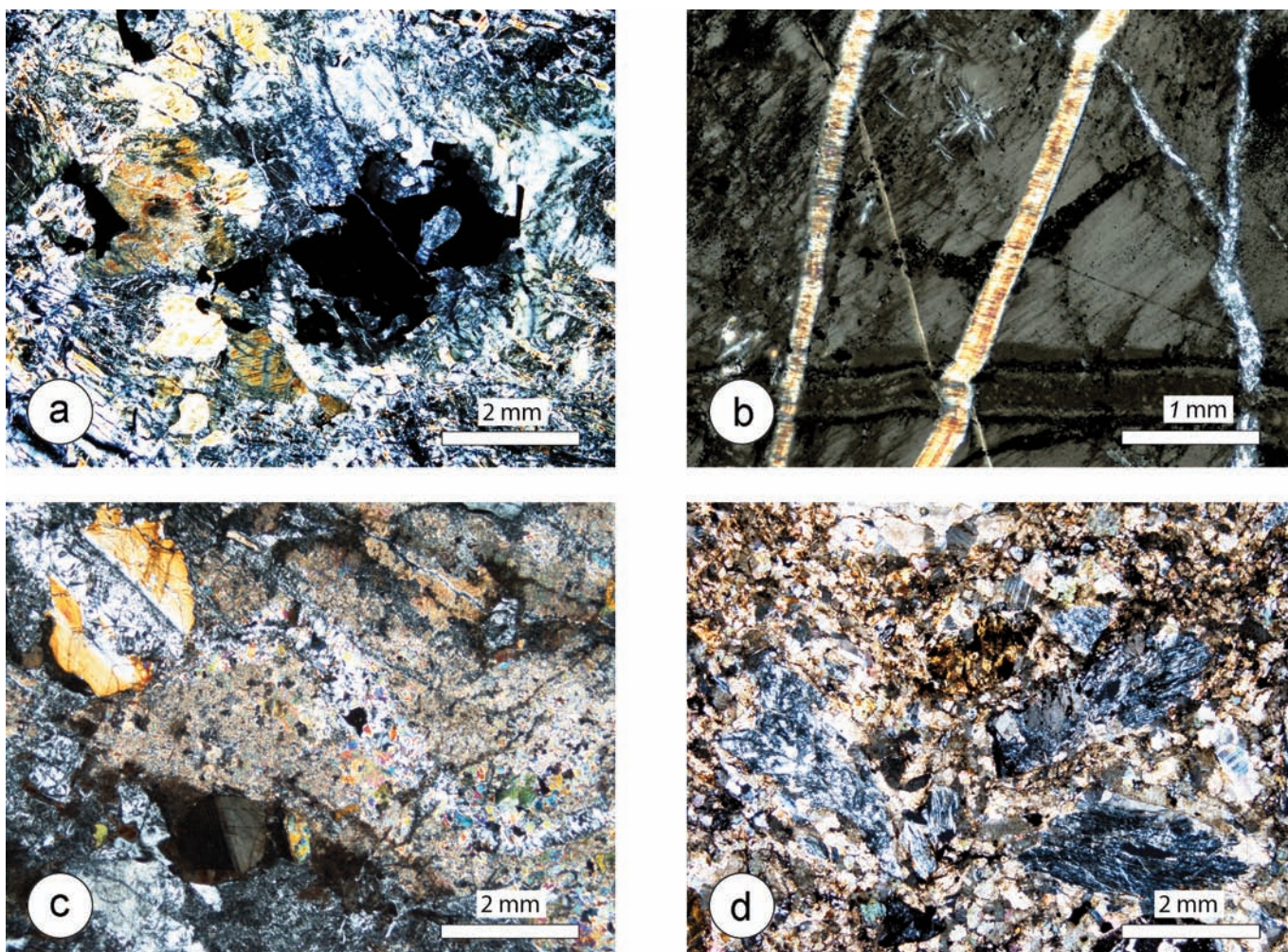


Fig. 3 - Microphotographs of serpentinized peridotites from le Ville outcrop (a), crysotile fibrous veins in peridotites from Gineprone outcrop (b), rodingitized gabbros from Gineprone outcrop (cm) and cataclasites from le Ville outcrop (d).

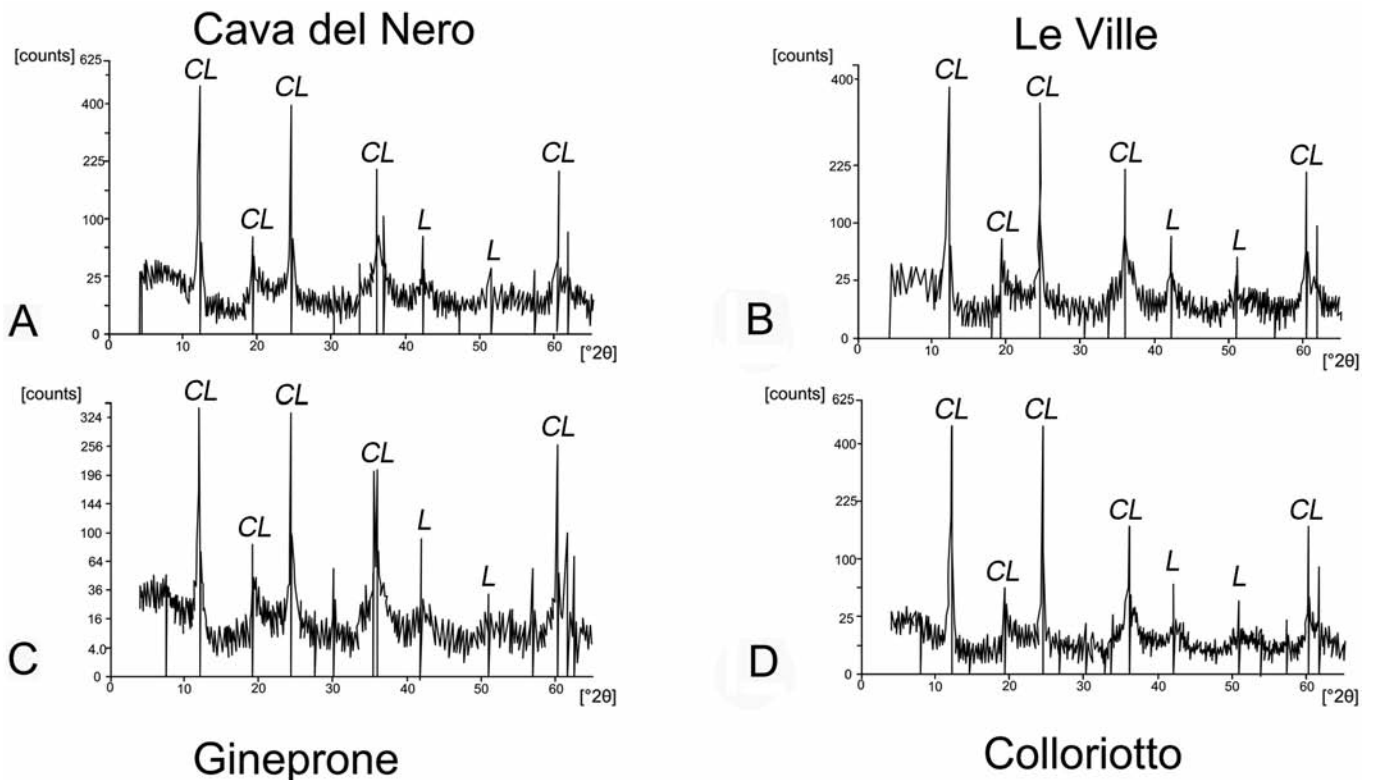


Fig. 4 - X-ray diffractograms of the serpentinites from Cava del Nero (A), Le Ville (B), Gineprone (C) and Colloriotto (D). For each peak the corresponding mineral is indicated: C - chrysotile; L - lizardite.

separated by lines of low birefringence, are irregular but reproduce the vein walls inside all the vein length. These veins commonly show median lines and bands of wall rock fragments parallel to the vein walls, that can be related to the inclusion bands of wall rock fragments described by Ramsay (1980) in calcite- and quartz-filled fibrous veins. All these features indicate that these veins were opened by crack and seal mechanism. Crack propagation is not driven by peridotite texture as demonstrated by bastite minerals cut across by veins.

The main difference among the peridotites from the four studied outcrops is the serpentinization degree. Peridotites affected by medium degree of serpentinization consists of scattered remnants of spinel and pyroxenes set in a serpentine groundmass consisting of bastite and mesh or hourglass textures after olivine. If the serpentinization is low, the primary tectonic porphyroclastic texture with well preserved pyroxenes and spinels in a poorly developed serpentine groundmass with mesh or hourglass structures after olivine is observed.

The rodingites derive from the interaction of gabbro dikes with hot, Ca-rich fluids in the oceanic environment (Tribuzio et al., 2004 and quoted references). The primary mineralogy of the gabbro is modified into an association of diopside, calcite and chlorite (Fig. 3c). No garnets and no veins have been observed. These rocks have been considered as peridotites for the calculation of the volume percentages, in order to place the estimation in the worst conditions.

The cataclasites consist of more than 60% of angular fragments of peridotite derived by crushing of neighbouring rocks (Fig. 3d), set in a matrix made up of calcite. No veins have been observed in these rocks. The fragments of peridotites show the same features of the host ones. In order to place the estimation in the worst conditions, these rocks

have been considered for the calculation of the volume percentages as the surrounding peridotites.

#### XRPD analyses

The serpentine group includes different silicates, among them the most common are antigorite, lizardite and chrysotile polymorphs, all recognized in the peridotites from Internal Ligurian Units (Mellini and Viti, 1994; Viti and Mellini, 1996; 1997; Donatio et al., 2009; Botti et al., 2010). Among the different polymorphs, the chrysotile shows commonly a fibrous habit, but may also occur in more massive microcrystalline aggregates (e.g., Wicks and O'Hanley, 1988). Lizardite is always observed as massive and microcrystalline aggregates (Mellini and Zanazzi, 1987; Mellini and Viti, 1994). Antigorite is generally found in non fibrous aggregates, but some varieties of this mineral can have been reported to be fibrous (e.g., Groppo and Compagnoni, 2007). Owing to their common T-O structural configuration, the superposition of the main diffraction peaks of the different polymorphs can occur. However, the peaks in the XRPD diffractogram of chrysotile and antigorite are well identifiable whereas the peak of chrysotile can be overprinted by those of lizardite (e.g., Biittner and Saager, 1982).

To characterize the peridotites from the Pievescola area, four samples of peridotites, one for each outcrops, have been analyzed by XRPD analysis (Fig. 4). In all the analyzed samples the occurrence of minerals belonging to the serpentine group has been detected. The identification of the minerals has been done according to the diffraction values reported by Whittaker and Zussman (1955) for minerals subjected to XRPD. The detected *d* values (Fig. 4) indicate the occurrence of both chrysotile and lizardite, whereas the antigorite is virtually lacking.



### IR index determination

The selected samples analyzed to determine the IR index have been chosen as representative of the lithology of the different outcrops, taking into account the calculated volume percentages.

The peaks between 3651 and 3620 cm<sup>-1</sup> are selected in order to estimate the IR index (Pucci et al., 2006). The area of the band included between the two peaks is thus calculated. This area is representative of the chrysotile percentage in the sample and a linear regression is made on each standard result. The instrument calibration must cover the values of chrysotile between 5 and 80%.

The IR Index result is shown in the Fig. 5. The values of the IR are comparable with a range from 0.14 to 0.21. The IR values are in agreement with the macro- and microscopic observations, i.e., the highest values correspond to the most serpentinized or more veined samples. Concerning the study area, all the IR values determined for the analyzed samples are slightly greater than the limit defined as dangerous by the Ministerial Decree 14/05/1996.

### Model of airborne dispersion of asbestos fibers

Geologic data, both from field analyses and laboratory activity, have been used for to model of the atmospheric dispersion of asbestos fibers, induced by a simulated quarrying activity in the study area. A simulation was performed for each outcrop, using the software MATLAB r2010a.

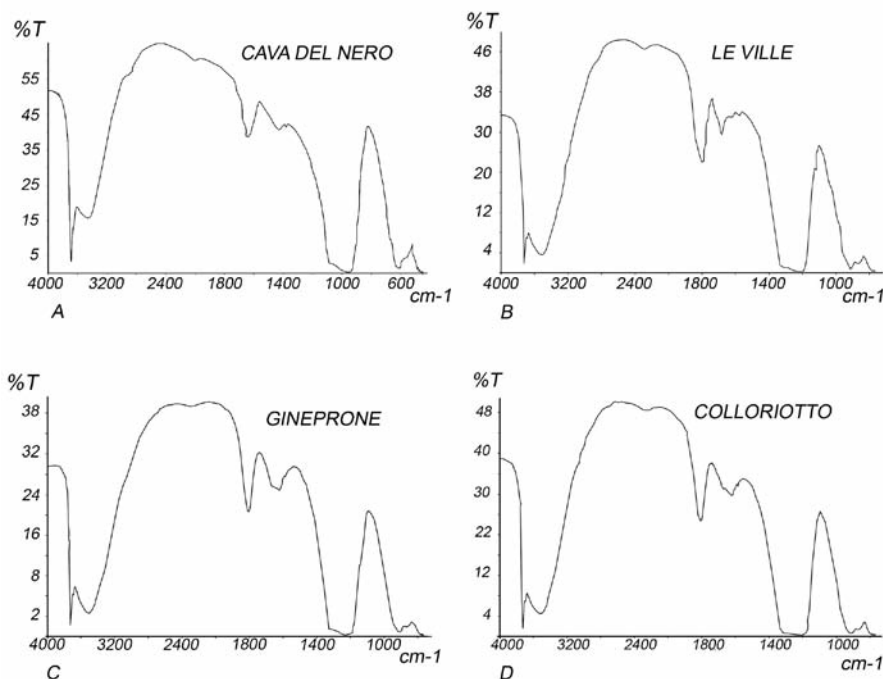
Preliminarily, the modelling requires an estimate of the flow rate of extraction (Q) during a simulated and hypothetical quarry activity. The hypothesized activity includes blast-

ing of the quarry fronts and removal of the resulting materials by quarry equipments, represented by two excavators and two dumpers. In our hypothesis, the modelling concerns a continuous activity (24 hours/day) in a week for a total of 168 hours. In 168 hours of quarry activity an extraction of 200.000 kg is scheduled. This value is a mean, taking into account the ordinary work time tables in a quarry always active. This value is adopted in order to place the modelling in the worst conditions, i.e., values three times those of a normal quarry operation, where 8 hours of activity are normally scheduled. The asbestos fibers are represented only from a part of total extracted mass (A%), calculated by IR analysis.

The following equation estimates the flow rate extraction of fibers (expressed as grams for hour) in the modelling:

$$(1) Q = \frac{(200 \cdot 10^3) \cdot [A\%]}{168}$$

In addition, the modelling needs several further inputs: atmospheric stability classes, area morphology, plume height, emission rate, prevailing wind velocity and direction. The atmospheric stability classes have been obtained from Pasquill atmospheric stability tables (Pasquill, 1961), based on location of the site, the wind velocity and the day period. The assignment of the classes allows the use of the stability coefficients, representative of atmospheric characteristics of the site. The area morphology has been loaded in the model has a DEM file. The plume height has been estimated as a constant value of 30 meters (e.g., Chaulya et al., 2001). This value has been calculated as a mean of the heights reached by the fibers after detonations. The Aeronautica Militare provided velocity and direction wind data for a timespan of 30 years (1961-1990).



Outcrop	% Asbestos released	% Relative density	IR Index
Cava del Nero	23.90	126.00	0.19
Le Ville	14.70	92.00	0.16
Colloriotto	15.68	112.00	0.14
Gineprone	18.90	115.00	0.21

Fig. 5 - Diagrams and related asbestos released percentage, relative density percentage and IR index of the serpentinites from Cava del Nero (A), Le Ville (B), Gineprone (C) and Colloriotto (D).



Such data have been written in text files, one for each month of simulation. In each text file every value has been written a number of times equal to its frequency of wind velocity and direction value. Every time steps the model chooses a value of these parameters through a random function. The grid value represents the size of the model calculation grid. It is necessary to find a value that represents a balance between the accuracy of the calculation and the computational timing.

The governing equation for the model is the Gauss dispersion into the atmosphere equation:

$$(2) \quad C(x, y, z) = \frac{Q}{7200\pi u \sigma_y \sigma_z} \exp\left\{-\frac{1}{2} \frac{y^2}{\sigma_y^2} - \frac{1}{2} \frac{z^2}{\sigma_z^2}\right\}$$

where:

C is the concentration of the fibers on the ground (expressed as grams for square meter);

Q is the fibers flow rate of extraction;

u is the velocity of the wind (m/s);

$\sigma_y$  and  $\sigma_z$  are the dispersion coefficients, which depend on the Pasquill classification system.

This equation refers to gas dispersion and it has been corrected with Stokes law to take into account the gravitational sedimentation rate. This correction makes effective the Gauss equation for the behaviour modelling of particulate in a fluid. To use the Stokes law, the cylindrical asbestos fibers have been treated as spheres. Regarding the reliability of the modelling, the approximation of the asbestos fibers to spheres is able to introduce a relevant error (up to 50%) in the modelling. To minimize this error, the equivalent aerodynamic diameter has been calculated using the slip correction factor by Cunningham (1910) that approximate the behaviour of a sphere to that of a cylinder, i.e., a shape like that of asbestos fibers (e.g., Allen and Raabe, 1985). Stoke law expresses the force of viscous friction to which it is subjected a sphere, which moves with respect to a fluid with a Reynolds number less than 1. This law allows the calcula-

tion of the gravitational sedimentation velocity, that represents the fibers behaviour in atmosphere.

The Gauss equation needs that the X-axis has the same orientation of the wind direction for each model time step. The coordinate system is the Cartesian one with the x axis oriented in the west-east direction and the y axis in the south-north direction. The unit of measurement is meter.

The equations 3 provide the correct orientation to the reference system the correct orientation. During the computation the coordinate system is rotated to coincide the x axis with the wind direction:

$$(3) \quad dw = \frac{(270 - dor)\pi}{180}$$

where:

dw is the direction of the wind for the calculation;

dor is the real direction of the wind.

The equation provides the modification of the position of the source and of the receptor.

$$\begin{aligned} x &= x \cos(dw) + y \sin(dw) \\ y &= y \cos(dw) - x \sin(dw) \end{aligned}$$

The wind in the Gaussian expression is the mean value that controls the plume extension. However, an exponential is required to obtain the wind velocity at to the desired height, keeping constant the direction, because the available meteorological data are collected at soil. In the effective height calculation, the wind velocity at the source height is used. The model has been applied for all outcrops, but in this study is reported only Cava del Nero example. The model provides in output a graph (Fig. 6) where the spatial distribution of the concentration of fibers to the ground after one year of quarrying is provided. After the simulation the obtained results have been exported from MATLAB and imported in ArcGIS to created a thematic mapping (Fig. 6).

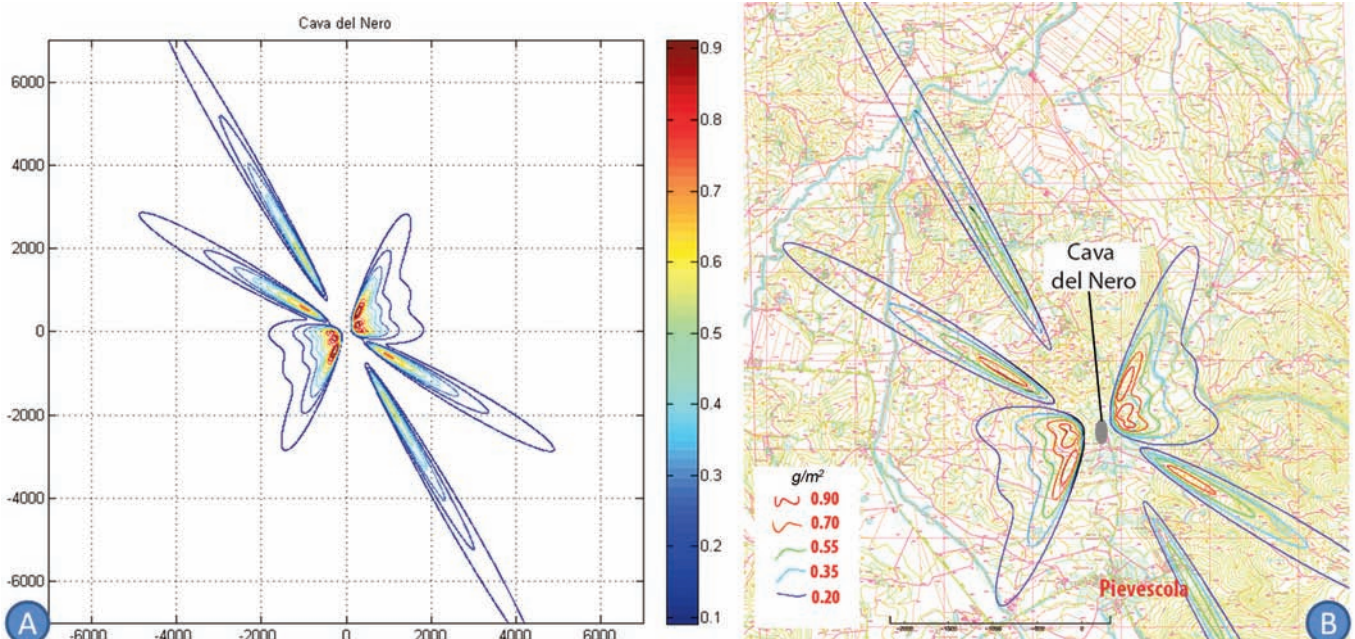


Fig. 6 - A: Spatial dispersion of asbestos fibers released from Cava del Nero after one year of mining activity. B: Spatial dispersion of asbestos fibers released from Cava del Nero after one year of mining activity plotted on the topographical map.

## DISCUSSION

In this study, we propose an approach based on five steps in order to evaluate the asbestos-related hazard induced by quarrying or excavation activity. These steps comprises: 1) the structural mapping associated to the identification of all the lithotypes in selected outcrops representative of the area to be investigated; 2) the petrographical analyses, 3) the XRPD analyses; 4) the IR determination and, finally, 5) the modelling of airborne dispersion of asbestos fibers.

This approach is simple, it does not requires special techniques and can be performed using standard equipment. Therefore, it represents a good and easy-to-use tool for engineers and geologists.

The first step is the most critical one, mainly because its aim is the identification of all lithotypes that can be regarded as asbestos-bearing and, at the same time, the assessment of their volume percentage. The final goal is not only to identify the asbestos-bearing lithotypes (mainly peridotite vs fibrous veins) but also to create a virtual sample representative of the whole studied outcrop. This virtual sample will be the material to analyze for the IR determination. This point deserves special attention, mainly because the collection of the sample can produce very different results from the IR determination depending on the criteria how the sample is collected. Moreover, further uncertainties concerning how the outcrops reflect the total volume of the asbestos-bearing rocks that is not exposed. Whereas the correct estimation of the volume percentage of the different lithotypes can be probably improved by the accurate use of techniques of structural mapping, the relationships between the field observations with the not exposed occurrences rock volume can be probably best estimated by a drilling program, able to provide a picture until a depth of several tens of meters. The identification of standard procedures for the structural mapping to be adopted by a Ministerial Decree can be regarded as a fundamental improvement for the IR determination.

The second and third steps can be achieved by standard petrographical and mineralogical techniques in petrography and mineralogy. The microscale observation of the veins allows to provide a clear picture of the occurrence of serpentine minerals with fibrous or non fibrous habit, but it prevents the discrimination of the different mineral species belonging to serpentine group. In this study, the analyses of eight thin sections are adequate to detect the serpentine min-

erals characterised by fibrous morphology. This discrimination can be performed by XRPD analyses. In the XRPD diffractogram, the peak of antigorite is well distinguishible from those of chrysotile and lizardite, that are generally overlapping. However, these minerals are characterized by different habits; antigorite and chrysotile can be characterized by fibrous habit whereas the lizardite occurs as massive and microcrystalline aggregates. Therefore, the crosscheck by of these two methods allows a precise characterization of the serpentine minerals. In this study, the microscopic and the XRPD analyses of the peridotite samples have been able to determine the occurrence of both lizardite and chrysotile, with the latter characterized by fibrous habit. Further studies, as microRaman spectroscopy (Groppo et al., 2006), can be integrated into the third step to solve more complex occurrences. However these analyses require more advanced techniques, and therefore can be time consuming.

The IR determination, is crucial for the proposed model, and for any attempt of asbestos hazard evaluation. The IR determination is affected by some uncertainties as suggested in several papers (Belardi et al., 2008; Bellopede et al., 2009). Beside the problems induced by the sampling strategy, the IR determination is affected by uncertainties represented by the absence of standard procedures about the calculation of the material density. This lacking makes the density values poorly comparable among different laboratories. For instance, in some laboratories the density is obtained from predetermined tables, as specified in the legislation. In contrast, others laboratories experimentally measure the density values. It is important to outline the positive correlation among the estimation of serpentinization degree, the IR index and the volume percentage measurements of the fibrous veins (Fig. 7). The highest value of the IR index has been detected in the samples collected in the Gineprone quarry, where the serpentinization degree is medium and the highest percentage of fibrous veins has been measured. In contrast, the Colloriotto outcrop, where the lowest percentage of fibrous veins has been detected and the serpentinization degree is low, provides the samples with lowest IR index. This evidence indicates that during the crushing of serpentinites the asbestos fibers are mostly provided by fibrous veins, whose occurrence strongly influences the IR index. The lacking of linear correlation between IR index and the estimate percentage of fibrous veins can be interpreted as the result of the problems in the collection of representative samples for IR index.

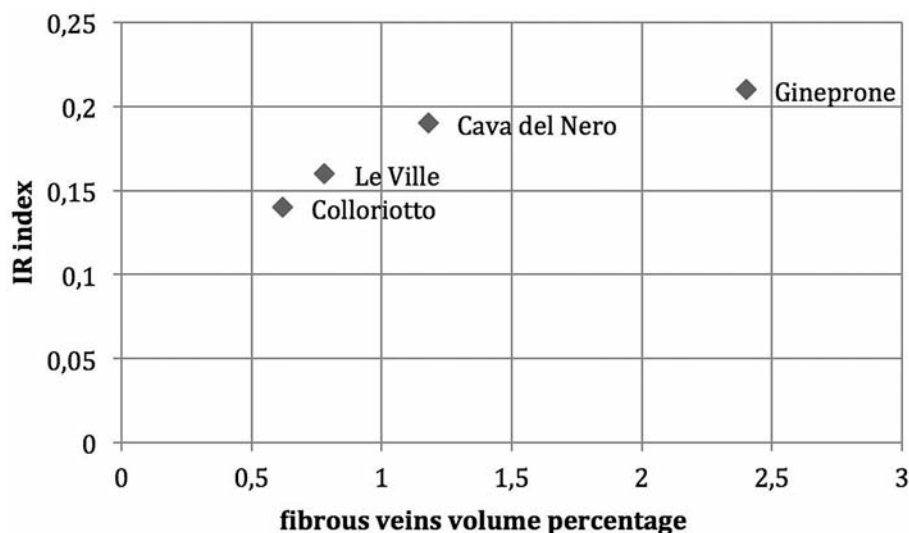


Fig. 7 - Correlation between the between the IR index and the volume percentage measurements of the fibrous veins.



All the data from the field and the laboratory analyses, have been used for the numerical modelling of the dispersion of the asbestos fibers in the atmosphere caused by a quarrying activity. The model, realized with the software MATLAB, takes into account not only the field and laboratory analyses but also others parameters as the values of wind direction and velocity chosen from a frequency matrix with a random function, the area morphology from the DTM file and the flow rate of fibrous material, calculated on the basis of experimental data of flow rate of extraction (Q) and the IR values. For the simulation in the model, the virtual site has been collocated in the Cava del Nero outcrop, but it can be applied to all the studied outcrops. The result of the modelling indicates that the concentration of the fibers to the ground varies according to several factors, first of all the morphology of the area. This implies that the quarries located at an altitude lower than the surrounding land, for example the Gineprone outcrop, generate small areas of fall-out deposits, but with very high concentration of fibers to the ground. In contrast, the area of dispersion is greater for the outcrops at greater altitude than the surrounding areas.

The main problem is the lacking for the study area of specific wind data, that are able to change deeply the results. Thus, an anemometer network in the study area would be necessary to improve the modelling with reliable local wind direction and velocity data. In our modelling the lacking of these data has been solved by applying corrective formulas, that take into account the morphology and climate characteristics of the area. However, the availability of local data is crucial to provide a more realistic modelling. In contrast, the variations flow rate of extraction (Q) causes less relevant effects in the modelling results than, for instance, the ones caused by the morphology. The variation of one order

of magnitude of the flow rate of extraction (Q) does not change substantially the concentration of fibers to the ground.

## CONCLUSIONS

The purpose of this paper is to define an approach that integrates field and laboratory analyses with modelling, to obtain an evaluation of the asbestos-related hazard induced by quarrying activity in asbestos-bearing serpentinites. The importance of this hazard assessment is demonstrated by the several papers that have been recently devoted to this topic (e.g., Cortesogno et al., 2005; Giacomini et al., 2010; Vignaroli et al., 2011; Gaggero et al., 2013). The approach adopted in this paper consists of 5 successive steps as described in the flow chart of Fig. 8. These steps include: of 1) the detailed structural mapping with the aim to collect samples representative of the cropping out rocks, 2) the petrographical study of selected thin sections of serpentinites with the aim to assess the presence of fibrous minerals, 3) the XRPD analyses for the identification of the species of fibrous minerals, 4) the determination of the IR according to the Ministerial Decree 14/05/1996 in order to determine the release of fibrous minerals by the asbestos-bearing rocks and 5) the modelling of the airborne dispersion of asbestos fibers by the quarrying activity based on the data collected in the previous steps.

According to the simulation performed in the Pievescola area, this integrated approach can be regarded as effective, even if liable of improvements. Particularly, the procedures adopted in this approach must be furtherly tested on several areas representative of different topographical and geological conditions, in order to optimize both field

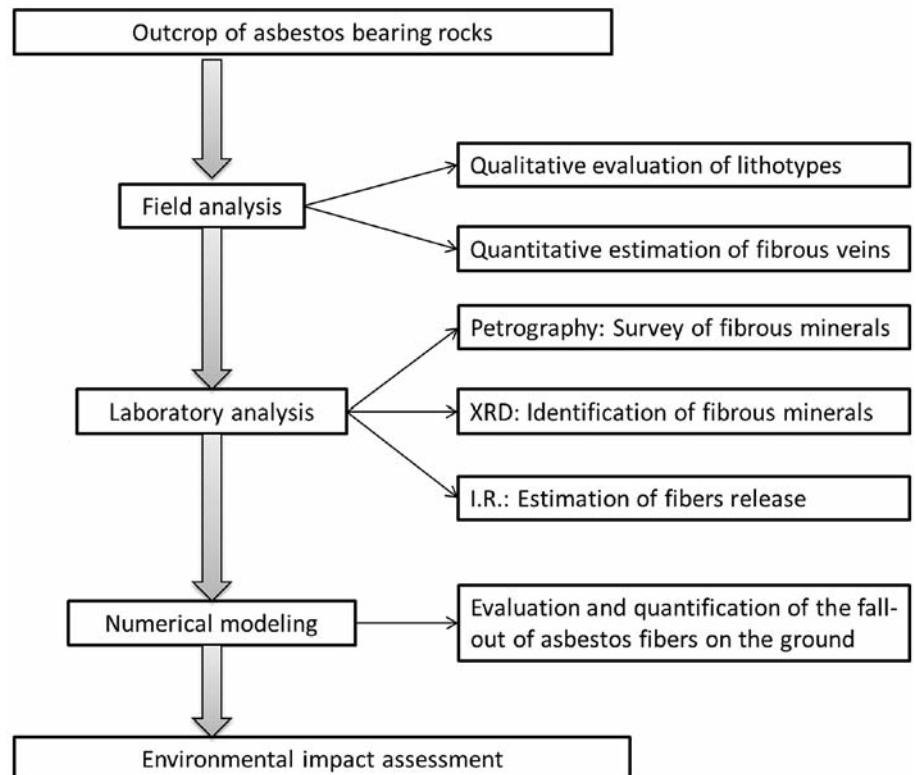


Fig. 8 - Flow charts of the adopted approach.

and laboratory analyses as well as the resulting modelling. Anyway, the goal of this paper is that to provide useful suggestions to make more effective the present-day legislation concerning the assessment of the asbestos-related hazard.

### ACKNOWLEDGEMENTS

The authors gratefully acknowledge two anonymous reviewers. The authors are indebted to Carlo Gini for XRPD analyses assistance. The Centro di Geotecnologie of Siena University is also acknowledged for the IR analyses.

### REFERENCES

- Allen M. and Raabe O., 1985. Slip correction measurements of spherical solid aerosol-particles in an Improved Millikan Apparatus. *Aerosol Sci. Technol.*, 4: 269-286.
- Annuario statistico regionale, 2010. Regione Toscana: <http://www.regione.toscana.it/-/annuario-statistico-regionale-toscana> 2010.
- Belardi G., Spaziani E. and Passeri L., 2008. La prova di automacinazione secondo il D.M. 14 maggio 1996: analisi degli effetti prodotti dalle principali variabili operative sulla curva granulometrica ottenuta a seguito del test. *Geingegneria Ambientale e Mineraria*, GEAM, 44 (2): 5-21.
- Bellopede R., Clerici C., Marini P. and Zanetti G., 2009. Rocks with Asbestos: Risk evaluation by means of an abrasion test. *Am. J. Env. Sci.*, DOI:<http://www.doaj.org/doaj?func=openurl&genre=article&issn=1553345X&date=2009&volume=5&issue=4&spage=500>
- Botti F., Donatio D., Gemelli M., Marroni M., Pandolfi L. and Rocchi S., 2010. Occurrence of fibrous minerals from Northern Apennine ophiolites: comparison among three different tectonic settings. 85<sup>th</sup> Congr. Naz. Soc. Geol. It. Rend. Soc. Geol. It., 12: 460-461.
- Biittner W. and Saager R., 1982. Rapid XRPD Determination of the Chrysotile/Lizardite ratios in Asbestos-bearing serpentinites. *Tscherm. Min. Petr. Mitt.*, 30: 177-187.
- Catanzariti R. and Perilli N., 2011. Chronostratigraphic framework of the External Ligurian Units (Late Cretaceous; Northern Apennines; Italy) based on calcareous nannofossils. *Ophioliti*, 36 (1): 37-57.
- Cattaneo A., Cavallo D.M. and Foà V., 2006. Patologia umana conseguente all'inalazione di fibre di asbesto. *Rend. Soc. Geol. It.*, 3: 37-40.
- Chaulya S.K., Chakraborty M.K. and Singh R.S., 2001. Air pollution modelling for a proposed limestone quarry. *Water Air Soil Poll.*, 126: 171-191.
- Cunningham E., 1910. On the velocity of steady fall of spherical particles through fluid medium. *Proc. Roy. Soc.* 83: 357; doi:10.1098/rspa.1910.0024
- Cortosogno L., Gaggero L. and Molli G., 1994. Ocean floor tectono-metamorphic evolution in the Piedmont-Ligurian Jurassic basin: a review. *Mem. Soc. Geol. It.*, 48: 151-163.
- Cortosogno L., Gaggero L., Marescotti P. and Robbiano A., 2005. Naturally occurring asbestos minerals from metaophiolites: rationales for custom-designed analytical constraints. AMAM 2005: Asbestos monitoring and analytical methods-amam 2005, Abstr. Vol., p. 83.
- Doll R., 1955. Mortality from lung cancer in asbestos workers. *Br. J. Ind. Medicine*, 12: 81-86.
- Donatio D., Marroni M. and Rocchi S., 2009. Ophiolitic rocks from Northern Apennine as a source of mineral fibers: preliminary comparison between Internal and External Ligurian Units, FIST Geitalia 2009, Abstr. Vol., 03-9: 116.
- Gaggero L., Crispini L., Isola E. and Marescotti P., 2013. Asbestos assessment in natural and anthropic ophiolitic environments: case studies of geohazard from northern Apennine ophiolites (eastern Liguria). *Ophioliti*, 38(1): 29-40.
- Giacomini F., Boerio V., Polattini S., Tiepolo M., Tribuzio R., and Zanetti A., 2010. Evaluating asbestos fibre concentration in metaophiolites: a case study from the Voltri Massif and Sestri-Voltaggio Zone (Liguria, NW Italy). *Environ. Earth Sci.*, 61: 1621-1639.
- Groppo C. and Compagnoni R., 2007. Ubiquitous fibrous antigorite veins from the Lanzo Ultramafic Massif, Internal Western Alps (Italy): characterisation and genetic conditions. *Per. Mineral.*, 76: 169-181.
- Groppo C., Rinaudo C., Cairo S., Gastaldi D. and Compagnoni R., 2006. Micro-Raman spectroscopy for a quick and reliable identification of serpentinite minerals from ultramafics. *Eur. J. Mineral.*, 18: 319-329.
- Hughes J.M. and Weill H., 1991. Asbestosis as a precursor of asbestos related lung cancer: results of a prospective mortality study. *Br. J. Ind. Medicine*, 48: 229-233.
- Italian Ministerial Decree, 1996. Laws and technical methods for remediation measures, including those for rendering asbestos harmless, as per Article 5(1)(f), of Law no. 257 of 27 March 1992, setting out: "Regulations related to the ban on using asbestos". Published in the Official J. It. Republic, 251, 25 October 1996, Ordinary Suppl., 178.
- Marinaccio A., Scarselli A., Binazzi A., Mastrantonio M., Ferrante P. and Iavicoli S., 2008. Magnitude of asbestos-related lung cancer mortality in Italy. *Br. J. Cancer*, 99 (1): 173-175.
- Marroni M., 1991. Deformation history of the Mt. Gottero Unit (Internal Liguride Units, Northern Apennines). *Boll. Soc. Geol. It.*, 110: 727-736.
- Marroni M., Molli G., Ottria G. and Pandolfi L., 2001. Tectono-sedimentary evolution of the External Liguride Units (Northern Apennine, Italy): insights in the precollisional history of a fossil ocean-continent transition zone. *Geod. Acta*, 14 (5): 307-320.
- Marroni M. and Pandolfi L., 2007. The architecture of the Jurassic Ligure-Piemontese oceanic basin: tentative reconstruction along the Northern Apennine - Alpine Corsica transect. *Int. J. Earth Sci.*, 96: 1059-1078.
- Marroni M., Meneghini F., and Pandolfi L., 2010. Anatomy of the Ligure-Piemontese subduction system: evidences from Late Cretaceous-Middle Eocene convergence-related deposits from Northern Apennines (Italy). *Int. Geol. Rev.*, 10-12: 1160-1192.
- Marroni M., Pandolfi L. and Meneghini F., 2004. From accretion to exhumation in a fossil accretionary wedge: a case history from Gottero Unit (Northern Apennines, Italy). *Geodin. Acta*, 17: 41-53.
- Mellini M. and Viti C., 1994. Crystal structure of lizardite-1T from Elba, Italy. *Am. Mineral.*, 79: 1194-1198
- Mellini M. and Zanazzi P.F., 1987. Crystal structures of lizardite-1T and lizardite-2H1 from Coli, Italy. *Am. Mineral.*, 72: 943-948.
- Mossman B.T., Bignon J., Corn M., Seaton A. and Gee J.B.L., 1990. Asbestos: scientific developments and implications for public policy. *Science*, 247: 294-301.
- Pasquill F., 1961. The estimation of the dispersion of windborne material. *Metereol. Mag.*, 90: 33-49
- Pucci M., Petri M.T., Gerra C., Marabino A.M., Plescia P., Tocino M.A. and Paoloni G., 2006. Pietrischi ferroviari da rocce verdi: metodologia d'analisi del contenuto d'amianto e metalli pesanti e suggerimenti per una corretta valutazione del potenziale inquinante. *Argomenti*, 8: 75-102
- Ramsay J.G., 1980. The crack-seal mechanism of rock deformation. *Nature*, 284: 135-139.
- Singhal B.B.S. and Gupta R.P., 2010. Applied hydrogeology of fractured rocks. Springer Verlag, 2<sup>nd</sup> Ed., 408 pp.
- Strohmeier B.R., Huntington J.C., Bunker K.L., Sanchez M.S., Allison K. and Lee R.J., 2010. What is asbestos and why is it important? Challenges of defining and characterizing asbestos. *Int. Geol. Rev.*, 52: 801-872.



- Treves B. and Harper G.D., 1994. Exposure of serpentinites on the ocean floor: sequence of faulting and hydrofracturing in the Northern Apennine ophiolites. *Ophioliti*, 19: 435-466.
- Tribuzio R., Thirwall M.F. and Vannucci F., 2004. Origin of the gabbro-peridotite association from the Northern Apennine ophiolites (Italy). *J. Petrol.*, 45 (6), 1109-1124.
- Vignaroli G., Rossetti F., Belardi G. and Billi A., 2011. Linking rock fabric to fibrous mineralisation: a basic tool for the asbestos hazard. *Nat. Hazards Earth Syst. Sci.*, 11: 1267-1280.
- Viti C. and Mellini M., 1996. Vein antigorites from Elba, Italy. *Eur. J. Mineral.*, 8: 423-434
- Viti C. and Mellini M., 1997. Contrasting chemical composition in coexisting lizardite and chrysotile from Elba veins. *Eur. J. Mineral.*, 9: 585-596.
- Virta R.L., 2002. Asbestos. U.S. Geol. Survey Open-File Rep., 02 (149): 1-49.
- Wagner J.C., 1991. The discovery of the association between blue asbestos and mesotheliomas and the aftermath. *Br. J. Ind. Medicine*, 48: 399-403.
- Whittaker E.J.W. and Zussman J., 1955. The characterization of serpentine minerals by X-ray diffraction. *Mineral. Mag.*, 31(233): 107-126.
- Wicks F.J. and O'Hanley D.S., 1988. Serpentine minerals: structures and petrology. In: S.W. Bailey (Ed.), *Hydrous phyllosilicates (exclusive of micas)*. *Rev. Mineral.* 19: 91-167.
- Wicks F.J. and Whittaker E.J.W., 1977. Serpentine textures and serpentinization. *Can. Mineral.*, 5: 459-488.

Received, March 4, 2013

Accepted, May 23, 2013